Adsorption of pNIPAM Layers on Hydrophobic Gold Surfaces, Measured in Situ by QCM and SPR

Mark A. Plunkett,[†] Zhehui Wang,[‡] Mark W. Rutland,[†] and
Diethelm Johannsmann*,[‡]

*Department of Chemistry, Surface Chemistry, Royal Institute of Technology,
SE-100 44 Stockholm, and The Institute for Surface Chemistry, P.O. Box 5607,
SE-11486 Stockholm, Sweden, and Max-Planck Institute for Polymer Research,
Ackermannweg 10, 55128 Mainz, Germany*

In situ surface plasmon resonance (SPR) and quartz crystal microbalance (QCM) measurements have been employed to measure the adsorption kinetics and absolute adsorbed amount of the poly(*N*-isopropyl acrylamide) (pNIPAM) from bulk aqueous solution onto a hydrophobized gold substrate. The adsorption was carried out at 31 °C, which is just below the lower critical solution temperature of pNIPAM in water. We find that the shift in the coupling angle of the surface plasmon (proportional to the "optical thickness") and the shift in the resonance frequency of the quartz crystal (proportional to the "acoustic thickness") increase in parallel for most of the adsorption. Also, the change of dissipation is proportional to the change in frequency. These observations suggest that the buildup of the polymer layer proceeds via growth in thickness rather than by densification of a layer with constant thickness. We interpret this finding in the sense that the dense high-temperature phase wets the hydrophobic gold surface. The wetting layer has a fixed density and grows in thickness. In addition, the QCM has been used to study the temperature-induced conformational change for pNIPAM around the critical temperature. It was found that the technique was able to monitor additional adsorption that occurs when crossing the critical point, which was due to bulk phase separation. Desorption was also noted when crossing the critical point from the opposite direction, and for the given system the process was entirely reversible.

Introduction

Interest in the poly(*N*-isopropyl acrylamide) (pNIPAM) system stems from the fact that it has a fully reversible lower critical solution temperature (LCST) in water at around 31 °C.[1] Because this temperature lies between room temperature and body temperature, it is foreseen that pNIPAM could be of interest in biological applications. Above the critical temperature, the polymer phase separates from solution, while below, the polymer becomes soluble. The LCST is a result of the entropy gain for the dehydration of the amide moieties with increasing temperature and can be affected by additives such as salt, alcohol, and surfactants and by the variation of the solution pH.[2] When attached to a solid surface, the pNIPAM layer swells and deswells with the temperature. In this way, one can tune the thickness of the layer and its softness.[3] Gels of pNIPAM show temperature-induced shape transformations, which makes them useful as sensors or actuators.[4]

In this paper, we are interested in the properties of pNIPAM layers physisorbed to solid substrates. To gain structural information on these layers, we combined surface plasmon resonance (SPR)[5] measurements with a quartz crystal microbalance (QCM).[6,7] Both techniques are capable of monitoring the kinetics of adsorption. However, the two techniques are sensitive to different aspects of the process, and hence the in situ comparison can lead to a greater understanding of the mechanisms. For example, SPR probes a certain combination of the thickness and refractive index, sometimes also termed the "ellipsometric moment" of the density profile.[8] The ellipsometric moment is largely (but not strictly) proportional to the adsorbed amount. The QCM, on the other hand, probes a combination of the acoustic impedance and thickness, which can be termed the "acoustic moment". Importantly, the QCM is sensitive to any adsorbed mass, including solvent, associated with the films. We elaborate on this difference on a mathematical basis in the Theory section. In addition, the QCM provides information on the dissipation inside the layer and, hence, on its viscoelastic properties.

Materials

In this investigation, we have monitored the adsorption of the temperature-sensitive pNIPAM onto a hydrophobic substrate. The substrate was a gold-coated quartz crystal, which was hydrophobized by the self-assembly of dodecanethiol. Such self-assembled monolayes provide a reliable and convenient way to form stable hydrophobic surfaces. pNIPAM was purchased from Polymer Source, Inc., and was reported to be of an average molecular weight

* Author for correspondence. Phone: + 49-5323-72 3768. Fax: + 49-5323-72 4835. E-mail: johannsmann@pc.tu-clausthal.de.
† Royal Institute of Technology and The Institute for Surface Chemistry.
‡ Max-Planck Institute for Polymer Research. Present address: Institute of Physical Chemistry, Arnold-Sommerfeld-Str. 4, 38678 Clausthal-Zellerfeld, Germany.

(1) Schild, H. G. *Prog. Polym. Sci.* **1992**, *17*, 163.
(2) Graziano, G. *Int. J. Biol. Macromol.* **2000**, *27*, 89.
(3) Arndt, K. F.; Kuckling, D.; Richter, A. *Polym. Adv. Technol.* **2000**, *11*, 496.
(4) Kuckling, D.; Vo, C. D.; Wohlrab, S. E. *Langmuir* **2002**, *18*, 4263−4269.

(5) See, for example: Knoll, W. In *Handbook of Optical Properties*; Hummel, R. E., Wibmann, P., Eds.; CRC Press: Boca Raton, FL, 1997; Vol. II, p 373.
(6) Höök, F.; Rodahl, M.; Brzezinski, P.; Kasemo, B. *Langmuir* **1998**, *14*, 729.
(7) Laschitsch, A.; Menges, B.; Johannsmann, D. *Appl. Phys. Lett.* **2000**, *77*, 2252.
(8) Charmet, J. C.; de Gennes, P. G. *J. Opt. Soc. Am.* **1983**, *73*, 1777.
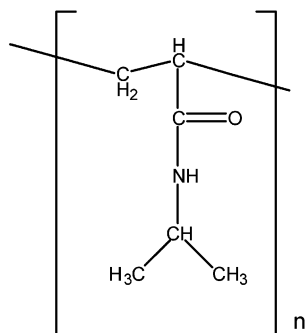
Figure 1. Schematic of the pNIPAM structure, where n is the degree of polymerization.

(M_w) of 275 kg/mol (determined via intrinsic viscosity measurements in methanol) with a polydispersity index of $M_w/M_n = 2.75$ (determined via size exclusion chromatography). pNIPAM was subsequently dialyzed with molecular weight cutoff 10 000 g/mol dialysis tubing to remove any possible low-molecular-weight contamination before being freeze-dried and stored, ready for use. The molecular structure of pNIPAM is represented in Figure 1.

Theory

The QCM[9-11] and SPR spectroscopy[5] are common techniques for measuring film thicknesses in the range a few monomolecular layers. Both techniques are based on the reflection of a wave at the substrate—film interface and share common principles.[12] The existence of standing waves in the layer system defines a resonance condition (frequency or coupling angle), the shift of which is used to probe film thickness during growth.

Provided that the layer is much thinner than the wavelength of light,[13] the shift of the plasmon coupling angle is to first order in film thickness given by[14]

$$\frac{n\omega}{c}\Delta(\sin\theta_c) = \Delta k_x \approx \frac{\omega}{c}\frac{2\pi}{\lambda}$$
$$\left(\frac{\epsilon_m\epsilon_a}{\epsilon_m + \epsilon_a}\right)^2 \frac{1}{(-\epsilon_m\epsilon_a)^{1/2}(\epsilon_a - \epsilon_m)}\frac{(\epsilon_f - \epsilon_a)(\epsilon_f - \epsilon_m)}{\epsilon_f}d_f \quad (1)$$

with n being the refractive index of the ambient medium,[15] θ_c the coupling angle, ϵ the dielectric constant, d_f the film thickness, and λ the wavelength. The indices "a", "f", and "m" denote the ambient medium, the film, and the metal substrate, respectively. Equation 1 can be generalized to account for continuous refractive index profiles, for example, created by a dilute adsorbate:

$$\Delta(\sin\theta_c) \approx \frac{2\pi}{n\lambda}\left(\frac{\epsilon_m\epsilon_a}{\epsilon_m + \epsilon_a}\right)^2 \frac{1}{(-\epsilon_m\epsilon_a)^{1/2}(\epsilon_a - \epsilon_m)} \times$$
$$\int_0^\infty \frac{[\epsilon_f(z) - \epsilon_a][\epsilon_f(z) - \epsilon_m]}{\epsilon_f(z)}\,dz \quad (2)$$

(9) Lu, C.; Czanderna, A. W., Eds. *Applications of Piezoelectric Quartz Crystal Microbalances*; Elsevier: Amsterdam, The Netherlands, 1984.
(10) Schumacher, R. *Angew. Chem., Int. Ed. Engl.* **1990**, *29*, 329.
(11) Johannsmann, D. *Macromol. Chem. Phys.* **1999**, *200*, 501.
(12) Höök, F.; Kasemo, B.; Nylander, T.; Fant, C.; Sott, K.; Elwing, H. *Anal. Chem.* **2001**, *73*, 5796.
(13) Lekner, J. *Theory of Reflection*; Kluwer Academic Publishers Group: Dordrecht, The Netherlands, 1987.
(14) Pockrand, I. *Surf. Sci.* **1978**, *72*, 577.
(15) When prism coupling is used instead of grating coupling, n is the refractive index of the prism.

where the integral is termed the "ellipsometric moment".[8] This is the quantity determined in any technique based on optical reflectometry, including ellipsometry and SPR spectroscopy. When working with metal surfaces, one can further assume that $\epsilon_f(z) - \epsilon_m \approx \epsilon_a - \epsilon_m$ and pull this quantity out of the integral, leading to

$$\Delta(\sin\theta_c) \approx \frac{2\pi}{n\lambda}\left(\frac{\epsilon_m\epsilon_a}{\epsilon_m + \epsilon_a}\right)^2 \frac{1}{(-\epsilon_m\epsilon_a)^{1/2}}\int_0^\infty\frac{\epsilon_f(z) - \epsilon_a}{\epsilon_f(z)}\,dz \quad (3)$$

We define the "optical thickness" d_{opt} as the thickness of an equivalent compact layer generating the same shift of the surface plasmon as the film under study. One has

$$d_{opt} = \Delta(\sin\theta_c)\left[\frac{\epsilon_{dry} - \epsilon_a}{\epsilon_{dry}}\right]^{-1}\left(\frac{2\pi}{n\lambda}\left(\frac{\epsilon_m\epsilon_a}{\epsilon_m + \epsilon_a}\right)^2\frac{1}{(-\epsilon_m\epsilon_a)^{1/2}}\right)^{-1} \quad (4)$$

where ϵ_{dry} is the dielectric constant of the adsorbate in its dry state. The parameters related to the film have been collected in the square brackets. The term in square brackets is a weight function, describing how strongly a film of a given thickness and dielectric constant affects the coupling angle.

Similar equations hold for quartz crystal resonators. In the long-wavelength limit ($d_f \ll \lambda$, λ the wavelength of shear sound), one has[16,17]

$$\frac{\delta f^*}{f} \approx -\frac{m_f}{m_q}\left[1 - \left(\frac{Z_q^2}{Z_f^2} - 1\right)\frac{Z_a^2}{Z_q^2}\right]$$
$$\approx -\frac{m_f}{m_q}\left[1 - \frac{Z_a^2}{Z_f^2}\right] = -\frac{m_f}{m_q}\left[\frac{Z_f^2 - Z_a^2}{Z_f^2}\right] \quad (5)$$

For convenience, eq 5 is again derived in the appendix. The quantity δf^* is the complex frequency shift $\delta f + i\,\delta\Gamma$, where f is the frequency and Γ is the half-band half-width (HBHW). m_f and m_q are the masses per unit area of the film and quartz plate, respectively. One has the relation $m_q = Z_q/(2f_0)$, with f_0 being the fundamental frequency. Z_a, Z_f, and Z_q are the acoustic impedances of the ambient medium (the liquid), the film, and the quartz, respectively. One has $Z_q = 8.8 \times 10^6$ kg m^{-2} s^{-1}. The acoustic impedance is given by $Z = (\rho G)^{1/2}$, with ρ being the density and G the shear modulus. The second line makes use of the relation $Z_q \gg Z_f$, which is true for soft adsorbates. In soft-matter experiments, G varies much stronger than ρ. The acoustic impedance is to a large extent governed by the material's shear modulus. For liquids, one has $G = i\omega\eta$, with $\eta = \eta' - i\eta''$ being the viscosity. The acoustic impedance is the acoustic analogue of the refractive index, and Z^2 is the analogue of the dielectric constant. Because eq 5 is linear in mass, it also holds in an integral sense:

$$\frac{\delta f^*}{f} \approx -\frac{1}{m_q}\int_0^\infty\left[\frac{Z_f^2(z) - Z_a^2}{Z_f^2(z)}\right]\rho(z)\,dz \approx$$
$$-\frac{\rho}{m_q}\int_0^\infty\left[\frac{G_f(z) - G_a}{G_f(z)}\right]\,dz \quad (6)$$

In the second line it was assumed that the density, ρ, is about constant. The integral could be called the "acoustic moment". The term in square brackets is again a weight

(16) Johannsmann, D. *Macromol. Chem. Phys.* **1999**, *200*, 501.
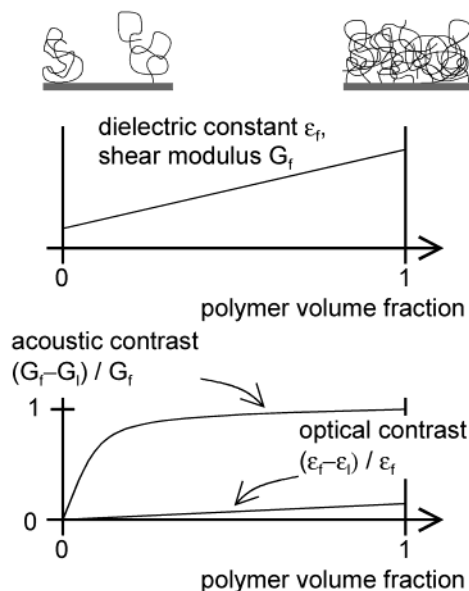(17) Johannsmann, D. *J. Appl. Phys.* **2001**, *89*, 6356.

Figure 2. Schematic illustration of the qualitative difference between optical and acoustic reflectometries. When a polymer layer of constant thickness grows in density, its optical contrast is roughly proportional to the polymer volume fraction. The acoustic contrast, on the other hand, saturates to a value of unity.

function, describing how much a film of given thickness and acoustic impedance affects the resonance frequency. We define the acoustic thickness d_{ac} as the thickness of a hypothetical compact layer ($G_f \gg G_a$) inducing the same frequency shift as the layer of interest:

$$d_{ac} = -\frac{\delta f}{f}\frac{m_q}{\rho} \qquad (7)$$

Equation 7 is the well-known Sauerbrey equation.[18] The acoustic thickness is the Sauerbrey mass divided by the density of the film.

Comparing eqs 4 and 7, one might assume that the information contained in the SPR and quartz crystal resonances should be essentially the same. However, this is very often not the case. First, the contrast in acoustics is usually much larger than that in optics. While refractive indices generally vary in the range of some percent, shear moduli may easily increase over orders of magnitude even for rather dilute adsorbates. In optics, the weight function (square brackets in eq 4) is smaller than unity and roughly proportional to the concentration. Therefore, the plasmon shift is approximately proportional to the *adsorbed amount*. In acoustics, on the contrary, the weight function (square brackets in eq 6) easily saturates to a value of 1 even for dilute adsorbates if the shear modulus of the adsorbate is much higher than the shear modulus of the liquid.[19] The acoustic thickness reaches the *geometric thickness* at rather low coverage and does not increase much further upon densification of the film by prolonged adsorption. More pictorially speaking, if the adsorbate drags some solvent along in its shear movement, the trapped amount of solvent appears as a part of the film[20] (Figure 2). Swelling, therefore, effectively increases the acoustic thickness, while it affects the optical thickness

to a much lesser degree. As a side remark, we note that a rough substrate can also lead to differences between the optical and the acoustic thicknesses,[21] though the effect of the roughness should be small here.

Methods

Both the SPR and the QCM experiments were conducted in situ, and as such, certain preparations of the substrate were needed before conducting the experiment. To perform SPR on the quartz crystal surface, the surface must be etched to create a surface corrugation grating for optical coupling. The grating was produced by reactive ion beam etching. A photoresist (MAP205 from Microresist) was spin-cast onto the quartz blanks to a thickness of about 120 nm. A 5-nm chromium layer had been evaporated onto the substrates to improve adhesion. A master grating with a pitch of 520 nm was produced by illuminating the photoresist with crossed laser beams of a He:Cd laser ($\lambda = 442$ nm).[22] The resulting structure was transferred to the quartz plates with an ion mill (RR.ISQ76 from Roth & Rau, Wüstenbrand, Germany). A mixture of CF_4 and O_2 (flow rates of 1.2 and 0.8 sccm, respectively) was applied to the surface at an average energy of 0.6 keV. Atomic force microscopy images showed that the resulting structures were rather rectangular with a depth of 40 nm peak-to-peak. This modulation depth was found to give optimal coupling for gold substrates immersed in water. As has been described previously, the surface plasmon coupling angle depends slightly on the depth of the grating.[23] With regard to *shifts* of the coupling angle upon adsorption of a surface layer, the depth is unimportant and eq 1 may be applied.

In principle, the grating can pose a problem to the QCM measurements because water can be trapped in the troughs. The amount of trapped water may change upon polymer adsorption, for instance, when the trapped water is replaced by trapped polymer. Note, however, that the grating is very shallow. The aspect ratio is 13. As a result, trapping of water is only expected in the corners of the grating, not over the entire trough. Also, the grating does not cover the entire surface of the plate. Still, the presence of surface corrugation is expected to reduce the apparent acoustic thickness. When the apparent acoustic thickness is larger than the optical thickness, this means that the acoustic thickness corrected for the effects of surface corrugation would be even larger.

A gold layer ($\sim$100 nm with a 2-nm chromium adherent layer) is placed over the grating (maintaining the corrugation), which simultaneously acts as the QCM electrode and the SPR coupling layer. The back electrode was keyhole-shaped and much thicker (500 nm) than the front electrode to achieve energy trapping. The quartz was operated at its seventh harmonic at 35 MHz. The seventh harmonic was used because it avoids adverse effects due to insufficient energy trapping (which is often found on low harmonics), on one hand, and the interference of anharmonic sidebands (which is found for high harmonics), on the other hand. The resonance frequency and bandwidth were determined by fitting resonance curves to the conductance spectra.

Adsorptions were conducted from Milli-Q water at 31 °C. This temperature was chosen because it lies just below the critical point and, hence, maximizes adsorption without causing a phase separation in the bulk. The phase transition temperature of our particular material was around 32 °C, as was determined by monitoring the desorption of a thick, spin-cast pNIPAM film in water upon lowering the temperature from above the phase transition temperature. Before introduction of pNIPAM to the system, baselines for both the QCM and the SPR were measured in Milli-Q water. At time equal to 0, the polymer was introduced at a bulk concentration of 20 ppm and the adsorption process was monitored simultaneously by both techniques. The concentration of 20 ppm is small enough to avoid the precipitation of the bulk material. Low concentrations are also desirable to avoid the turbidity of the solution when the phase transition is

(18) Sauerbrey, G. *Arch. Elektrotech (Übertragung)* **1964**, *18*, 617.
(19) Domack, A.; Prucker, O.; Rühe, J.; Johannsmann, D. *Phys. Rev. E* **1997**, *56*, 680.
(20) Martin, S. J.; Frye, G. C.; Ricco, A. J. *Anal. Chem.* **1993**, *65*, 2910.

(21) Daikhin, L.; Urbakh, M. *Faraday Discuss.* **1997**, *106*, 27.
(22) Mai, X.; Moshrefzadeh, R.; Gibson, U. J.; Stegeman, G. I.; Seaton, C. T. *Appl. Opt.* **1985**, *24*, 3155.
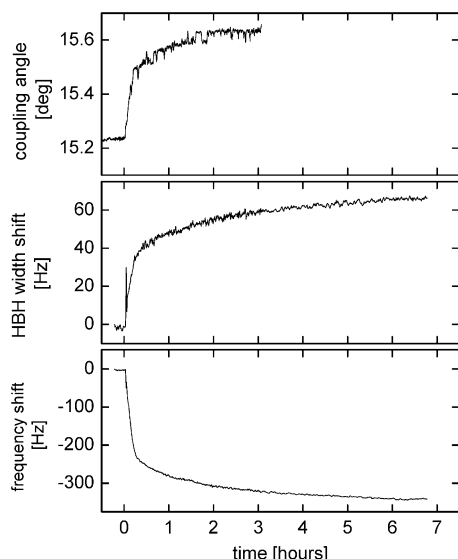(23) Fischer, B.; Fischer, T. M.; Knoll, W. *J. Appl. Phys.* **1994**, *75*, 1577.

Figure 3. Surface plasmon coupling angle, frequency shift, and HBHW as a function of the adsorption time (adsorption temperature: 31 °C).

approached. For turbid solutions, the reflectance minimum of the SPR curve becomes broad.

The effect of temperature on the conformation of pNIPAM is interesting; however, because quartz crystals are affected by variations in the temperature we must remove the inherent crystal effects from the measured response to investigate the effect of the temperature on the preadsorbed polymer layer. This was achieved by measuring the inherent temperature effects on the crystal prior to the addition of polymer to the system. The temperature was linearly cycled, up and down, between 24 and 36 °C in Milli-Q water. It was noted that for a constant rate of temperature change that there was a reproducible hysteresis between the increasing and decreasing temperature runs for the frequency. We believe this hysteresis to be related to stress in the holder. This interpretation is corroborated by the fact that the dissipation does *not* show hysteresis. Stress (like temperature) affects the frequency much more than the dissipation. The rate of increase and decrease in the temperature was kept constant at 12 °C/hr in these measurements. At this rate, the dissipation showed no hysteresis, being a roughly linear variation over the explored temperature range.

To minimize the effect of phase separation in the system, the bulk fluid was exchanged with twice the volume of Milli-Q water prior to the temperature variation measurements. To find the effect of the polymer on the complex frequency change, the corresponding temperature variation measurements were subsequently made after the adsorption of the polymer. To remove the effect of the hysteresis, all measurements were conducted at the same rate of temperature increase and decrease. The polymer-related complex frequency change was then determined by subtracting the calibration (no polymer) result from that obtained in the presence of the polymer. We emphasize that the term "polymer related" in this context can include an increased viscosity of the bulk in addition to polymer adsorption.

Results

Adsorption at 31 °C. A hydrophobized gold substrate was kept in contact with Milli-Q water at 31 °C until both the QCM and the SPR signals were stable. A baseline was recorded for both instruments simultaneously, before the introduction of polymer to the system, and the resulting adsorption was monitored. The results of the adsorption are shown in Figure 3, where the changes are plotted in both the resonant frequency (δf) and HBHW (δHBHW or $\delta\Gamma$) from the QCM as well as the SPR coupling angle as a function of time as a direct comparison of the adsorption
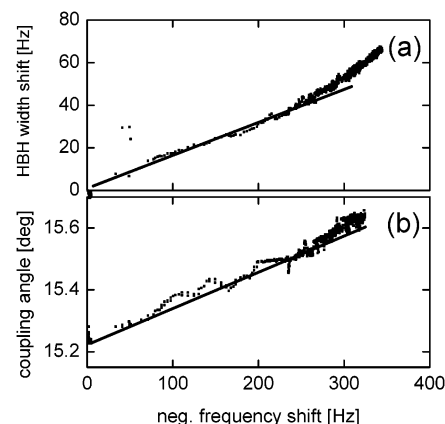

Figure 4. (a) HBHW (proportional to the dissipation) and (b) SPR coupling angle versus negative frequency shift $-\delta f$ for the adsorption of pNIPAM onto a hydrophobized gold surface as a function of time. The linear relation observed at low coverage suggests a thickness growth mode.

kinetics. The final frequency shift of -340 Hz corresponds to a Sauerbrey thickness (eq 7) of 10 nm; the shift in the coupling angle of 0.4° yields an optical thickness of 4 nm (eq 4). In the derivation of these numbers, a dn/dc of pNIPAM in water of 0.167 cm³/g (ref 24) and a bulk density of 1 g/cm³ was assumed. As usual, the acoustic thickness exceeds the optical thickness.

The apparent kinetics, as measured by the three different parameters, is very similar. To remove time as a variable from the adsorption plot, it is possible to plot the QCM results as the change in energy loss ($\delta\Gamma$) versus the negative of the measured frequency change ($-\delta f$). As a first approximation, this is a good way to investigate the buildup of surface adsorbed layers in terms of conformation and viscoelasticity because it is a plot of the energy loss as a function of the adsorbed mass. This is shown in Figure 4a with a straight line included to illustrate the linearity during the initial adsorption. A linear relation is also found in the plot of the surface plasmon coupling angle versus the frequency shift (Figure 4b). The surface plasmon coupling angle by and large reflects the adsorbed amount: It is not affected by trapped water.

Temperature-Induced Conformational Changes. Figure 5 shows the raw data for the effect of the temperature on the QCM responses of the crystal with and without adsorbed polymer. Panel a displays how the frequency response varies over a temperature range of 24−36 °C. There is a clear hysteretic effect even in the absence of polymer, which is attributed entirely to instrumental considerations. More complex hysteresis behavior is observed when the polymer is present in solution and adsorbed to the surface, and this is the convolution of the instrumental hysteresis and the polymer behavior. An additional complexity to the behavior is introduced by the fact that adsorption and desorption both occur depending on the direction of the temperature change. The dissipative behavior (Figure 5b) is considerably simpler because there is no instrumental hysteresis in this case.

The instrumental contribution to the frequency and dissipation changes can be accounted for simply by subtracting them from the respective polymer cases, and the result of this treatment is shown in Figure 6. A simple bin averaging technique was employed. (This subtraction does not account for the increased viscosity of the bulk caused by the presence of the polymer.) It is now much
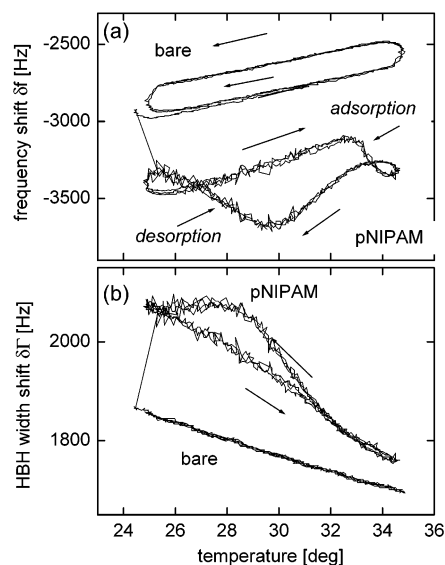
(24) Gao, J.; Wu, C. *Macromolecules* **1997**, *30*, 6873.

Figure 5. (a) Frequency shift δf versus temperature and (b) shift of HBHW $\delta \Gamma$ versus temperature for a preadsorbed layer of pNIPAM.
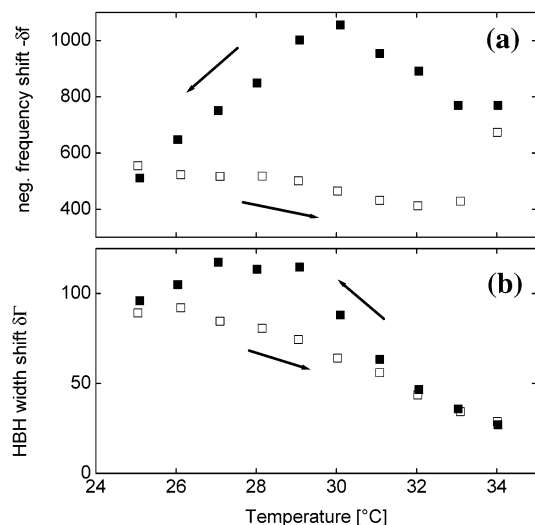

Figure 6. Change in (a) frequency and (b) dissipation associated with the adsorption of pNIPAM as a function of temperature.
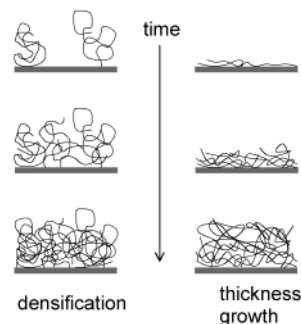

Figure 7. Schematic description of the limiting cases of the densification growth mode and the thickness growth mode.

simpler to interpret the behavior. Figure 6a shows how the frequency shift varies with the temperature. As the temperature is raised from 25 °C, the acoustic thickness ("mass") decreases slowly up to about 32 °C (approximately the LCST) after which it rises steeply. Two competing processes are at work. Below the LCST, the adsorbed

polymer is gradually collapsing and releasing solvent, whereas at the LCST, the dissolved polymer becomes insoluble and deposits onto the surface, leading to a sudden mass increase. (A decreased viscosity of the bulk caused by a collapse of the chains in the bulk would have the opposite effect.) Interestingly, the reverse process follows a different path. A *further* increase of the acoustic thickness occurs. Most likely, the deposited polymer swells as the solvent quality improves. Then, at a temperature below the LCST (30 °C), there is a decrease in the acoustic thickness with decreasing temperature as the excess polymer desorbs, so that finally the layer returns at 25 °C to the same state.

This argument is supported by the complementary dissipation data in Figure 6b. The dehydration/collapse of the polymer with increasing temperature from 25 °C is observed as a steady decrease in the dissipation. Interestingly, the dissipation appears insensitive to the deposition of polymer at 32 °C. However, the subsequent swelling of the layer is clearly observed as the temperature is decreased and once again is relatively insensitive to the mass change as the polymer desorbs.

Discussion

The performance of a polymer-bearing surface is directly related to the conformation of the adsorbed polymers. For instance, extended polymer cushions are soft and permeable to small molecules, whereas collapsed layers modify the chemical nature of the surface but are mechanically and hydrodynamically inactive. As a general rule, a strong adsorption favors a pancake conformation of collapsed chains, whereas weak adsorption leads to a more extended structure. Given a final thickness of the adsorbed layer of 10 nm, as was inferred from the frequency shift, one would conclude that pNIPAM is weakly adsorbed and forms a soft, extended polymer cushion. The thickness of the adsorbed layer is comparable to the radius of gyration, R_g, although it is somewhat difficult to put down exact numbers for R_g because of the rather large polydispersity of the material.

The growth mode of such dilute layers is usually thought to be a densification process.[25] Initially, the coverage is low. The adsorbed molecules have few attachment sites and remain Gaussian coils with little disturbance of their structure by the interface. As more and more chains adsorb, the interface gets crowded. This growth mode is different from the layer-by-layer thickness growth mode, where the first chains adopt a flat conformation and subsequent chains then deposit as pancakes on top of these chains.

Interestingly, our data indicate a *thickness growth mode*, rather than a densification process (Figure 7). This interpretation is based on two findings: the fact that optical and acoustic thicknesses go parallel and the fact the frequency shift and dissipation are largely parallel as well. We first argue why an acoustic thickness proportional to the optical thickness is not expected for the densification mode. The acoustic thickness and optical thickness differ in their contrast function, which are $(G_f - G_a)/G_f$ for the acoustic thickness and $(\epsilon_f - \epsilon_a)/\epsilon_f$ for the optical thickness. The dielectric constant typically varies by a few percent, whereas the shear modulus may vary by orders of magnitude if polymer strands are added to a liquid. As a

(25) Fleer, G. J.; Cohen Stuart, M. A.; Scheutjens, J. M. H. M.; Cosgrove, T.; Vincent, B. *Polymers at Interfaces*; Chapman and Hall; London, 1993.

consequence, the contrast function in optics is by and large proportional to the density, whereas the term $(G_f - G_a)/G_f$ comes close to unity for moderate polymer concentrations and does not increase much upon further increase of the polymer volume fraction (Figure 2). The acoustic contrast saturates. Were the film to grow via densification, one would expect the acoustic thickness to increase rapidly in the early phases of adsorption and remain constant later on, as part of the trapped water is replaced by polymer chains. This is not the case.

The comparison of the frequency shift and shift in HBHW leads to the same conclusion. The frequency and bandwidth are proportional to each other for the first hour of adsorption. This suggests that the viscoelastic properties of the film remain unchanged during the film growth. Strictly speaking, this statement only applies to the combination of parameters $Im[(G_f - G_a)/G_f]/Re[(G_f - G_a)/G_f]$. However, it is quite unexpected that the viscoelasticity should change in such a way that this ratio remains constant.

There is some deviation from linearity in the final stages of adsorption. While one might attribute these changes to variations in the viscoelasticity of the material (caused by densification), this is not necessarily the case. Equation 6 was calculated for the long-wavelength limit, that is, for layers much thinner than the wavelength of sound. The penetration depth of shear sound in water at $f = 35$ MHz is 60 nm, which is larger but not much larger than the final film thickness of 10 nm. For films that are thinner but not much thinner than the wavelength of sound, there is a perturbation calculation giving higher order corrections to $\delta f^*/f$ in the areal mass density m_f.[17] This calculation predicts

$$\frac{\delta f^*}{f} \approx -\frac{m_f}{m_q}\left[1 - \left(\frac{Z_q^2}{Z_f^2} - 1\right)\frac{Z_a^2}{Z_q^2}\right] + \left(\frac{m_f}{m_q}\right)^2\left[1 - \left(\frac{Z_q^2}{Z_f^2} - 1\right)in\pi\frac{Z_a}{Z_q}\right] \quad (8)$$

For the real part of $\delta f^*/f$, the second-order term in eq 8 can safely be ignored. For the imaginary part, however, this is not the case. The ratio $n\pi m_f/m_q/(Z_a/Z_q)$ quantifying the relative importance of the second-order term is about 7%. The curvature seen at high coverage in Figure 4a may be attributed either to a change of the viscoelastic properties of the layer or to a violation of the long-wavelength approximation and the corresponding second-order correction. However, closer inspection of Figure 4a shows that the data do not lie on a parabola. Rather, there is a kink at $\delta f \sim -250$ Hz, which would give support to the idea that the viscoelastic properties of the layer change for high adsorbed amounts. Such an observation has previously been made in a related experiment.[26]

A layer buildup via thickness growth seems counterintuitive because it is not clear why a layer-by-layer growth should stop at a film thickness equal to the diameter of the unperturbed chain. We argue that this peculiar growth mode is caused by the fact that the adsorption is done close to the LCST, where phase separation into a polymer-rich and a solvent-rich phase is imminent. We interpret our findings as a *wetting phenomenon*. The hydrophobic gold surface favors the polymer-rich phase and induces
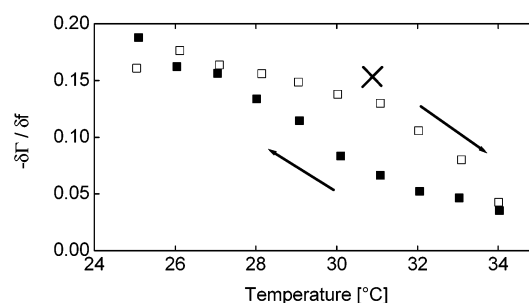
(26) Plunkett, M. A.; Claesson, P. M.; Rutland, M. W. *Langmuir* 2002, *18*, 1274.

Figure 8. Change in dissipation normalized by the negative change in frequency as a function of temperature.

the formation of a layer of this phase at its surface. Initially, the layer is rather flat. This pancake conformation is not primarily caused by a multitude of attachment sites; it is the consequence of the fact that there is phase boundary at the film−liquid interface. When the wetting layer grows in thickness, there is rearrangement of chain conformations, such that the chains arriving later also find points of attachment to the substrate. The rearrangement occurs under conditions of constant intramolecular interaction; the shape of the coils alters without an observable change in their viscoelastic properties. These rearrangements take time, making the adsorption a slow process. The growth of the wetting layer is arrested when the chains on top of the layer can no longer reach to the substrate. At this point, there is a slight decrease in the density, leading to the upward curvature in the $\delta\Gamma - \delta f$ plot and in the plot of optical versus acoustic thickness. The film does not grow to infinite thickness because we have a situation of *partial* wetting. Partial wetting often is the result of a delicate balance, in this case the temperature being just below the phase transition temperature.

To better understand the variation of the viscoelastic properties of the adsorbed film with temperature, we have plotted the dissipation normalized by the effective mass. Thus, we probe directly the change in viscoelastic properties. This is shown in Figure 8 for both the increasing (upper curve) and decreasing (lower curve) temperature traces. Not unexpectedly, there is a hysteresis between the two curves. We believe that this is due to the dynamics of the reconformation of the polymer layer being slower than the rate at which the temperature is changed.

We note that each point can be interpreted as the gradient of a $\delta\Gamma - \delta f$ plot such as in Figure 4a. In that figure, the adsorption was performed at constant temperature and the gradient (0.16) should, therefore, represent the equilibrium value for the ratio at that temperature. This point appears as a cross in Figure 8 and lies above both curves, suggesting that the layers have undergone some irreversible densification during the cycling process.

Summary

From the combined analysis of the in situ QCM and SPR measurements, we conclude that the adsorption of pNIPAM occurs by an increase in the thickness of the adsorbed polymer layer. Only in the final stages of the adsorption does there seem to be some deviation from this adsorption regime. The results indicate a consistent rigidity and solvent content over the majority of the adsorption, only slowly decreasing in rigidity in the final stages (final 30%) of the adsorption process.

The QCM technique is sensitive to any mass oscillating with the crystal, which includes hydrodynamically coupled
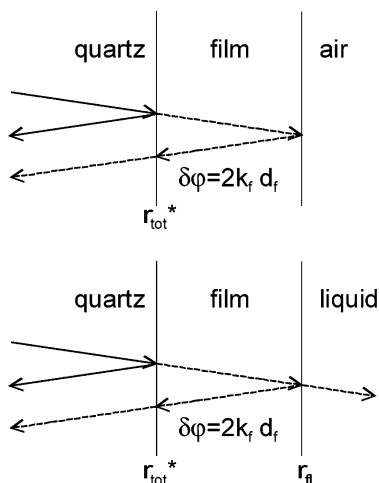
Figure 9. Schematic description of the acoustic model underlying the calculation of complex frequency shifts.

solvent. This is in contrast to the SPR technique that is dependent on the difference in the refractive indexes and is, thus, not sensitive to solvent contributions. It is, thus, a considerable advantage to run these techniques in parallel to gain a better understanding of the entire adsorption process, as is seen in these measurements. Contrast between different adsorption processes can, thus, be observed by measuring with the full range of techniques.

The effect of changing the temperature on the polymer conformation could also be investigated with QCM. This novel experiment demonstrates the possibility of running the QCM experiments as a function of the temperature by removing inherent temperature-dependent crystal responses. It was possible to determine separately the processes of adsorption/desorption, in addition to swelling/deswelling phenomena, for the pNIPAM system.

Appendix: Derivation of a Generalized Sauerbrey Equation for Films in Liquids

In the following, we provide a derivation of eq 5. A rigorous description of the acoustic modeling for the QCM is given in ref 16. Classically, the QCM is used to infer the areal mass density of a film via the Sauerbrey equation

$$\frac{\delta f}{f} = -\frac{2 f_0}{Z_q} m_f \tag{A1}$$

where δf is the frequency shift, f is the frequency, f_0 is the frequency of the fundamental, $Z_q = 8.8 \times 10^6$ kg m^{-2} s^{-1} is the acoustic impedance of the quartz plate, and m_f is the areal mass density. The Sauerbrey equation holds for films in air, provided that the film thickness is much less than the wavelength of sound.

For more complicated situations, one has to resort to acoustic modeling. We first rephrase eq A1, still assuming that the quartz is operated in air and that the acoustic properties of the film are the same as those of the quartz. One can then easily see that the fractional decrease in frequency is equal to the fractional increase in thickness of the quartz-film composite resonator. Using the wave picture, one can derive that the fractional frequency shift $\delta f/f$ is proportional to the phase shift $\delta\varphi = 2 k_f d_f$, acquired by the shear wave as it passes through the film (Figure 9):

$$\frac{\delta f}{f} = -\frac{\delta\varphi}{2\pi} = -\frac{2 k_f d_f}{2\pi} \tag{A2}$$

Here, k is the wavenumber, d is the thickness, and the index f labels the film.

In case the film's acoustic impedance is not the same as the acoustic impedance of quartz, one has to consider two reflected waves: the first one reflected at the quartz–film interface and the second reflected at the film–air interface. The complex coefficient of reflectivity, r, at an interface is given by $r = (Z_1 - Z_2)/(Z_1 + Z_2)$, where Z_1 and Z_2 are the acoustic impedances of the two materials. One can calculate an overall reflectivity at the quartz–film interface, r_{tot}, by either the matrix formalism or an iteration procedure, as described in Ref 27. The calculation proceeds in exactly the same way as the calculation of the reflectivities of optical multilayers, where the acoustic impedance takes the role of the refractive index. It turns out that the fractional frequency shift is given by

$$\frac{\delta f^*}{f} \approx i\frac{r_{tot}^* - 1}{2\pi} \tag{A3}$$

The asterisk (*) indicates complex quantities, where the complex resonance frequency is given by $f + i\Gamma$, with Γ the HBHW. Equation A3 is more general than eq A2. It accounts for the impedance mismatch and dissipation in the film. For thin films, the imaginary part of the reflection coefficient is the phase φ. In this limit, eq A2 is recovered.

An alternative treatment of the frequency shift in quartz resonators is possible in the frame of equivalent circuits and the transmission-line theory. In this context, it is helpful to define a generalized impedance via the relation

$$r^* = \frac{Z_q - Z^*}{Z_q + Z^*} \tag{A4}$$

Equation A4 is the usual condition for the reflection coefficient at interfaces with an impedance mismatch. If the medium contacting the quartz surfaces is a semi-infinite liquid, then Z^* is just the acoustic impedance of this liquid, $Z_l = Z^* = (i\omega\rho\eta)^{1/2}$. For more complicated situations, namely, layer systems, one defines Z^* as the ratio of stress, σ, and lateral speed, $\partial u/\partial t$, just above the quartz surface. Here, $u(z, t)$ is the displacement pattern of the acoustic wave. Z^* is *not* a material property like the acoustic impedance. It is defined in analogy to the electrical impedance, where stress takes the role of voltage and lateral speed takes the role of current. For a given equivalent circuit, Z^* is calculated from the individual circuit elements by application of the Kirchhoff rules.[28] Inserting eq A4 into eq A3 and assuming $Z_q \gg Z^*$ (which is true for most organic adsorbates), one finds

$$\frac{\delta f}{f_0} = \frac{i}{\pi}\frac{Z^*}{Z_q} \tag{A5}$$

Equation A5 is also proven by the application of the Thiersten equivalent circuit[29] in ref 30.

This leaves the problem of calculating the ratio of stress, σ, and lateral speed, $\partial u/\partial t$, just above the quartz surface for a viscoelastic film in a liquid. We write

(27) Azzam, R. M. A.; Bashara, N. M. *Ellipsometry and Polarized Light*; Elsevier: Amsterdam, 1987.

(28) Rosenbaum, J. F. *Bulk Acoustic Wave Theory and Devices*; Artech House: Norwood, MA, 1988; p 376.

(29) Thurston, R. N. In *Mechanics of Solids*; Truesdell, C., Ed.; Springer-Verlag: Heidelberg, 1984; Vol. 4, Chapter 36.

(30) Johannsmann, D.; Mathauer, K.; Wegner, G.; Knoll, W. *Phys. Rev. B* **1992**, *46*, 7808.

$$Z^* = \frac{\sigma}{\partial u/\partial t} = \frac{G_f \, \partial u/\partial z}{\partial u/\partial t} = \frac{G_f k(u^+ - u^-)}{\omega(u^+ + u^-)}$$

$$= \frac{G_f k(1 - u^-/u^+)}{\omega(1 + u^-/u^+)}$$

$$= Z_f \frac{1 - \exp(-2ik_f d_f)\dfrac{(Z_f - Z_l)}{(Z_f + Z_l)}}{1 + \exp(-2ik_f d_f)\dfrac{(Z_f - Z_l)}{(Z_f + Z_l)}} \quad (A6)$$

$$= Z_f \frac{(Z_f + Z_l)\exp(2ik_f d_f) - (Z_f - Z_l)}{(Z_f + Z_l)\exp(2ik_f d_f) + (Z_f - Z_l)}$$

Here, G_f is the shear modulus of the film and u^+ and u^- are amplitudes of the waves traveling in the forward and the backward directions. The indices "f" and "l" denote the film and the liquid, respectively. The term $(Z_f - Z_l)/(Z_f + Z_l)$ is the reflectivity of the film−liquid interface. The factor $\exp(-2ik_f d_f)$ accounts for the travel across the film. In the second line, we have used $G_f k_f/\omega = G_f(\rho_f/G_f)^{1/2} = (\rho_f G_f)^{1/2} = Z_f$. With eq A5, this translates to

$$\frac{\delta f^*}{f_0} = \frac{i}{\pi}\frac{Z^*}{Z_q} = \frac{i}{\pi}\frac{Z_f}{Z_q}\frac{(Z_f + Z_l)\exp(2ik_f d_f) - (Z_f - Z_l)}{(Z_f + Z_l)\exp(2ik_f d_f) + (Z_f - Z_l)} \quad (A7)$$

Equation A7 predicts the complex frequency shift for films of an arbitrary thickness in liquids. In case the film is much thinner than the wavelength of sound ("long-wavelength limit"), one may linearize the exponential and write

$$\frac{\delta f^*}{f_0} \approx \frac{i}{\pi}\frac{Z_f}{Z_q}\frac{(Z_f + Z_l)(1 + 2ik_f d_f) - (Z_f - Z_l)}{(Z_f + Z_l)(1 + 2ik_f d_f) + (Z_f - Z_l)}$$

$$\approx \frac{i}{\pi}\frac{Z_f}{Z_q}\frac{(Z_f + Z_l)ik_f d_f + Z_l}{(Z_f + Z_l)ik_f d_f + Z_f}$$

$$\approx \frac{i}{\pi}\frac{Z_f}{Z_q}\frac{[Z_l + (Z_f + Z_l)ik_f d_f][Z_f - (Z_f + Z_l)ik_f d_f]}{Z_f^2} \quad (A8)$$

$$\approx \frac{i}{\pi}\frac{Z_l}{Z_q} + \frac{i}{\pi}\frac{Z_f}{Z_q}\frac{(Z_f - Z_l)(Z_f + Z_l)ik_f d_f}{Z_f^2}$$

$$\approx \frac{i}{\pi}\frac{Z_l}{Z_q} - \frac{\omega m_f}{\pi Z_q}\frac{Z_f^2 - Z_l^2}{Z_f^2}$$

In the last line, we have used $Z_f k_f d_f = (\rho_f G_f)^{1/2}\omega(\rho_f/G_f)^{1/2} d_f = \omega m_f$. The first term in eq A8 is the frequency shift induced by the presence of the liquid. This term is absent when the quartz in the liquid is chosen as the reference state (assuming that the liquid used for the reference has the same viscosity as the liquid used in the experiment). With the $m_q = Z_q/(2f_0)$ and exchanging the index "l" for the index "a", eq A8 proves eq 5 in the main text.